

Multiplicity Scaling of Light Nuclei Production in Relativistic Heavy-Ion Collisions

Wenbin Zhao,¹ Kai-jia Sun,² Che Ming Ko,² and Xiaofeng Luo¹

¹*Key Laboratory of Quark and Lepton Physics (MOE) & Institute of Particle Physics,
Central China Normal University, Wuhan 430079, China*

²*Cyclotron Institute and Department of Physics and Astronomy,
Texas A&M University, College Station, Texas 77843, USA*

(Dated: March 1, 2022)

Using the nucleon coalescence model based on kinetically freeze-out nucleons from the 3D (2D) hybrid dynamical model, MUSIC (VISHNU), with a crossover equation of state (EOS), we study the multiplicity dependence of deuteron (d) and triton (t) production from central to peripheral Au+Au collisions at $\sqrt{s_{NN}} = 7.7, 14.5, 19.6, 27, 39, 62.4$ and 200 GeV and Pb+Pb at $\sqrt{s_{NN}} = 2.76$ TeV. It is found that the ratio $N_t N_p / N_d^2$ of the proton yield N_p , deuteron yield N_d and triton yield N_t exhibit a scaling behavior, i.e., decreasing monotonically with increasing charged-particle multiplicity. A similar multiplicity scaling of $N_t N_p / N_d^2$ is also found in the nucleon coalescence calculation based on nucleons from a multiphase transport (AMPT) model. The scaling behavior of $N_t N_p / N_d^2$ can be naturally explained by the size effects in the coalescence production of light nuclei, which is due to the interplay between the sizes of nuclei and nucleon emission source. Finally, we argue that the multiplicity scaling of $N_t N_p / N_d^2$ can serve as a baseline to search for possible QCD critical point and validate the production mechanism of light nuclei in relativistic heavy-ion collisions.

PACS numbers: 25.75.Ld, 25.75.Gz, 24.10.Nz

I. INTRODUCTION

Light nuclei production in high energy heavy-ion collisions have been extensively studied both experimentally and theoretically [1–15]. Besides its intrinsic interest, studying light nuclei production provides the possibility to probe the local baryon density and the space-time structure of the emission source in relativistic heavy-ion collisions [16–18]. However, the production mechanism for light nuclei in heavy-ion collisions is still under debate. On the one hand, the statistical model, which assumes that light nuclei, like hadrons, are produced from a thermally and chemically equilibrated source, provides a good description of measured yields of light (anti-)nuclei in central Pb+Pb collisions at Large Hadron Collider (LHC) [19–21]. On the other hand, the coalescence model, which assumes that light nuclei are formed from the recombination of kinetically freeze-out protons and neutrons [22–25], can also successfully describe the transverse momentum spectra and the collective flow of light nuclei in heavy-ion collisions [26–33]. In between above two extreme scenarios for light nuclei production in heavy-ion collisions is the transport model, which aims to study how light nuclei evolve during the hadronic evolution by including their production and annihilation, such as the processes $\pi + p + n \leftrightarrow d + \pi$ for the deuteron [34, 35]. In the latter study, it is assumed that the deuteron can exist in hot dense hadronic matter, although its temperature of more than 100 MeV is significantly higher than the deuteron binding energy of 2.2 MeV.

Recently, more experimental data on light nuclei production in relativistic heavy-ion collisions have become available. For example, the STAR Collaboration at Relativistic Heavy-Ion Collider (RHIC) and the ALICE Collaboration at the LHC have collected a wealth of data on

light nuclei, such as (anti-)deuteron (\bar{d} , d), (anti-)triton (\bar{t} , t) and (anti-)helium-3 (${}^3\bar{He}$, 3He), in Au+Au collisions from 7.7 GeV to 200 GeV and Pb+Pb collisions at 2.76 TeV, respectively [36–38]. A noteworthy result from these experiments is the observation that the yield ratio of triton, deuteron and proton, $N_t N_p / N_d^2$, in central Au+Au collisions all show a non-monotonic energy dependence with a peak around $\sqrt{s_{NN}} = 20$ GeV [37, 38]. A physically interesting explanation for this non-monotonic behavior is that it is due to the change in the QGP to hadronic matter phase transition from a crossover at small baryon chemical potential to a first-order transition at large baryon chemical potential and the large nucleon density fluctuations associated with the QCD critical point [39–44]. Another interesting observation from these experiments is the suppressed production of light nuclei in peripheral Au+Au collisions or in collisions of small systems. A possible explanation for this suppression is due to the non-negligible sizes of light nuclei compared to the size of the nucleon emission source [17, 45].

In this work, we investigate the multiplicity dependence of deuteron and triton production from peripheral to central Au+Au collisions at $\sqrt{s_{NN}} = 7.7 - 200$ GeV from Beam Energy Scan (BES) program at RHIC by using the nucleon coalescence model with the needed phase-space distribution of nucleons generated by the MUSIC or AMPT model. Specifically, nucleons at the kinetic freeze-out of the expanding hadronic matter in heavy-ion collisions are obtained from the hybrid approach MUSIC [46–49] or the AMPT [50] without having any fluctuation effects from dynamical QCD phase transitions. Since the hybrid model used in the present study has been shown to nicely reproduce the measured yield and collective flow of hadrons and light nuclei in heavy-ion collisions at both RHIC and LHC energies [31, 51], it

thus provides a robust baseline for the study of light nuclei production in the RHIC BES program [32, 51]. We find from our study that the yield ratio in collisions from $\sqrt{s_{NN}}=7.7$ GeV to 2.76 TeV is independent of the collision energy and decreases with increasing charged-particle multiplicity. Such a multiplicity scaling of this ratio contradicts to the prediction of the thermal model, which shows an opposite multiplicity dependence, i.e., an increasing with increasing charged-particle multiplicity [20, 21].

This paper is organized as follows: Section II briefly introduces the nucleon coalescence model and the MUSIC hybrid model. Section III presents and discusses results on the multiplicity dependence of the spectra, particle yield dN/dy , the coalescence parameters for deuteron and triton production, and the yield ratio $N_t N_p / N_d^2$ in Au+Au collisions at RHIC BES energies and in Pb+Pb collisions at LHC. Section IV concludes this paper with a summary.

II. THE THEORETICAL FRAMEWORK

A. The coalescence model for light nuclei production

In the coalescence model [22–25], the number of a light nucleus of atomic number A and consisting of Z protons and N neutrons ($A = Z + N$) is given by the overlap of the Wigner function f_A of the nucleus with the phase-space distributions $f_p(\mathbf{x}_i, \mathbf{p}_i, t)$ of protons and $f_n(\mathbf{x}_j, \mathbf{p}_j, t)$ of neutrons [24, 25],

$$\begin{aligned} \frac{dN_A}{d^3\mathbf{P}_A} &= \int \Pi_{i=1}^Z p_i^\mu d^3\sigma_{i\mu} \frac{d^3\mathbf{p}_i}{E_i} f_{p/\bar{p}}(\mathbf{x}_i, \mathbf{p}_i, t_i) \\ &\times \int \Pi_{j=1}^N p_j^\mu d^3\sigma_{j\mu} \frac{d^3\mathbf{p}_j}{E_j} f_{n/\bar{n}}(\mathbf{x}_j, \mathbf{p}_j, t_j) \\ &\times f_A(\mathbf{x}'_1, \dots, \mathbf{x}'_Z, \mathbf{x}'_1, \dots, \mathbf{x}'_N; \mathbf{p}'_1, \dots, \mathbf{p}'_Z, \mathbf{p}'_1, \dots, \mathbf{p}'_N; t') \\ &\times \delta^{(3)}\left(\mathbf{P}_A - \sum_{i=1}^Z \mathbf{p}_i - \sum_{j=1}^N \mathbf{p}_j\right), \end{aligned} \quad (1)$$

where $g_A = (2J_A + 1)/2^A$ is the statistical factor for A spin 1/2 nucleons to form a nucleus of angular momentum J_A . The \mathbf{x}_i and \mathbf{p}_i are coordinate and momentum of the i -th nucleon in the frame of the nucleon emission source, while \mathbf{x}'_i and \mathbf{p}'_i are those in the rest frame of the produced nucleus obtained from the coordinate \mathbf{x}_i and momentum \mathbf{p}_i by the Lorentz transformation.

Following Ref. [24], we take the Wigner functions of deuteron and triton to be Gaussian and using the same proton and neutron masses. For the deuteron, its Wigner function is then

$$f_2(\boldsymbol{\rho}, \mathbf{p}_\rho) = 8 \exp\left[-\frac{\boldsymbol{\rho}^2}{\sigma_d^2} - \mathbf{p}_\rho^2 \sigma_d^2\right], \quad (2)$$

with the relative coordinate $\boldsymbol{\rho}$ and the relative momentum \mathbf{p}_ρ defined as

$$\boldsymbol{\rho} = \frac{1}{\sqrt{2}}(\mathbf{x}'_1 - \mathbf{x}'_2), \quad \mathbf{p}_\rho = \frac{1}{\sqrt{2}}(\mathbf{p}'_1 - \mathbf{p}'_2). \quad (3)$$

For the triton, its Wigner function is

$$\begin{aligned} f_3(\boldsymbol{\rho}, \boldsymbol{\lambda}, \mathbf{p}_\rho, \mathbf{p}_\lambda) \\ = 8^2 \exp\left[-\frac{\boldsymbol{\rho}^2}{\sigma_t^2} - \frac{\boldsymbol{\lambda}^2}{\sigma_t^2} - \mathbf{p}_\rho^2 \sigma_t^2 - \mathbf{p}_\lambda^2 \sigma_t^2\right], \end{aligned} \quad (4)$$

with the additional relative coordinate $\boldsymbol{\lambda}$ and relative momentum \mathbf{p}_λ defined as

$$\boldsymbol{\lambda} = \frac{1}{\sqrt{6}}(\mathbf{x}'_1 + \mathbf{x}'_2 - 2\mathbf{x}'_3) \quad \mathbf{p}_\lambda = \frac{1}{\sqrt{6}}(\mathbf{p}'_1 + \mathbf{p}'_2 - 2\mathbf{p}'_3). \quad (5)$$

The width parameter σ_d in Eq. (2) is related to the root-mean-square radius r_d of deuteron by $\sigma_d = \frac{2}{\sqrt{3}}r_d$. Similarly, the width parameter σ_t in Eq. (4) can be related to the root-mean-square radius r_t of triton by $\sigma_t = r_t$. For the root-mean-square matter radius of deuteron and triton, we use the experimental values of $r_d = 1.96$ fm and $r_t = 1.59$ fm, respectively [52]. We note that because of the very small yields of deuterons and tritons in heavy-ion collisions at the RHIC BES energies, protons used in the coalescence processes have negligible effects on the final proton spectra.

It is worth to point out that there is an ambiguity of a prefactor in Eq.(1) for the three-body coalescence production of triton via $p+n+n \rightarrow t$. In Refs. [23–25], where nucleons are treated as classical particles, a prefactor of 1/2 is introduced to avoid double counting the neutrons in the production of tritons. This factor is, however, absent in Ref. [16]. According to Refs. [39, 43], without this factor the triton yield in the coalescence model using nucleons from a thermally and chemically equilibrated emission source is identical to that in the thermal model when the triton binding energy is neglected. In this work, we only consider the three-body coalescence channel for triton production and do not include a prefactor of 1/2 in Eq.(1) as in Refs. [16, 39, 43]. Compared to our previous study on triton production from the three-body channel in Ref. [32], which includes the prefactor of 1/2, both the triton yield and the double ratio, $N_t N_p / N_d^2$, at high multiplicity in this work will thus be about a factor of two larger.

B. The MUSIC hybrid model for heavy-ion collision dynamics

For the description of heavy-ion collision dynamics, we employ the MUSIC hybrid model [48, 51, 55–57]. The (3+1)D viscous hydrodynamics in MUSIC, which conserves both the energy-momentum and baryon number of produced QGP, is developed for describing its collective dynamics and the soft hadrons produced from the

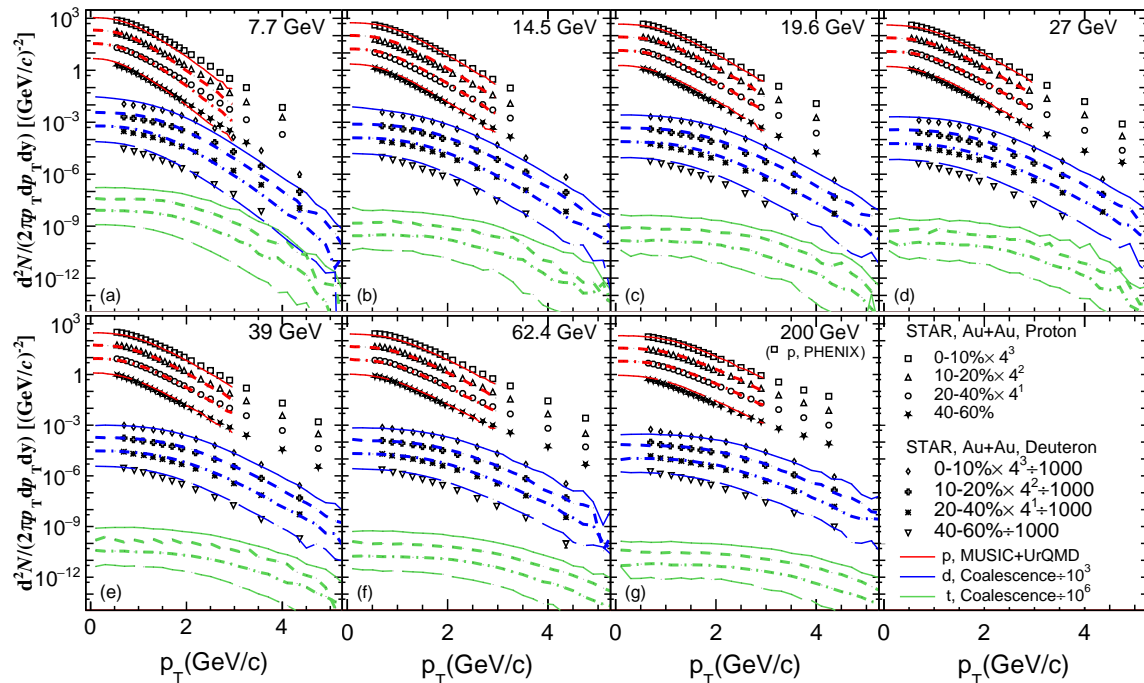


FIG. 1. (Color online) Transverse momentum spectra of protons, deuterons and tritons in Au + Au collisions at $\sqrt{s_{NN}} = 7.7, 14.5, 19.6, 27, 39, 62.4, \text{ and } 200 \text{ GeV}$. The data for deuterons are taken from the STAR Collaboration [37], and the data for protons are taken from the STAR and PHENIX Collaborations [53, 54].

hadronization hypersurface. At the RHIC BES energies, this hybrid model uses a smooth initial conditions and the net baryon density from an extended 3D Glauber model as the input for the subsequent hydrodynamic evolution [51]. For the present study, we use a crossover type of equation of state (EoS) (NEOS-BQS) with the strangeness neutrality condition of vanishing net strangeness density, $n_s = 0$, and the net electric charge-to-baryon density ratio $n_Q = 0.4n_B$ [58]. We use such an EoS without a QCD critical point because the aim of our study is to provide a reliable baseline calculation without any critical effects on light nuclei production in heavy-ion collisions at energies from the RHIC BES program. Following Refs. [51], we include in the hydrodynamic evolution a temperature and baryon chemical potential dependent specific shear viscosity η/s . After the hydrodynamic evolution, we convert fluid cells to hadrons when their energy densities drop below the switching energy density $e_{sw} = 0.26 \text{ GeV/fm}^3$. For the evolution and decoupling of the resulting hadronic matter, the MUSIC code switches to the microscopic hadron cascade model, UrQMD [59–61]. Finally, we obtain the phase-space distributions of kinetically freeze-out nucleons for the coalescence model calculations. We would like to emphasize that the MUSIC hybrid model employed in this paper has achieved a quantitative description of soft particle production, including the p_T -spectra and collective flow, in the central and peripheral Au+Au collisions at $\sqrt{s_{NN}} = 7.7 - 200 \text{ GeV}$, as demonstrated in Ref. [51]. This indicates that the MUSIC hybrid model can provide the proper phase-

space distributions of nucleons at the kinetic freeze-out for the coalescence model calculations.

III. RESULTS

In this section, we study the transverse momentum spectra, the rapidity distribution dN/dy , mean transverse momentum $\langle p_T \rangle$ as well as the multiplicity dependence of the coalescence parameters $A^{-1}\sqrt{B_A}$ ($A = 2, 3$) and the double yield ratio $N_t N_p / N_d^2$ of triton, deuteron and proton in Au+Au collisions at $\sqrt{s_{NN}} = 7.7 - 200 \text{ GeV}$.

A. Transverse Momentum Spectra and dN/dy

Figure 1 shows the transverse momentum spectra of protons, deuterons and tritons from central to peripheral Au+Au collisions at $\sqrt{s_{NN}} = 7.7, 14.5, 19.6, 27, 39, 62.4, \text{ and } 200 \text{ GeV}$. It can be found that the MUSIC hybrid model can quantitatively describe measured proton spectra¹ below 2.5 GeV but slightly underestimates the data at higher p_T , where the quark recombinations

¹ Note that the proton spectra in both STAR data and the model calculations have been corrected by subtracting the weak decay feed-down contributions. The weak decay feed-down correction for STAR's proton spectra reported in Ref. [53] is based on UrQMD+GEANT simulation.

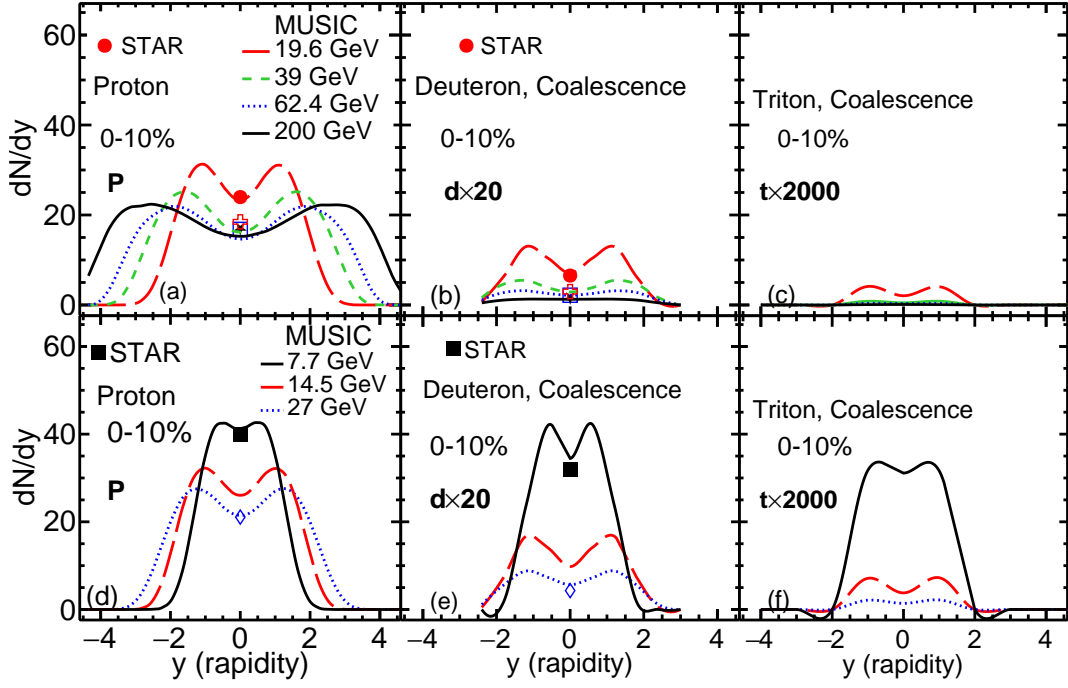


FIG. 2. (Color online) The rapidity distribution dN/dy of protons, deuterons, and tritons in 0-10% Au + Au collisions. The experimental data for protons and deuterons are taken from Refs. [37, 53, 54, 62].

contributions has been shown to gradually become important [63–69]. With the phase-space distributions of protons and neutrons at kinetic freeze-out from MUSIC, we calculate the spectra of deuterons and tritons within the framework of nucleon coalescence model. As shown with the blue lines in Fig. 1, without any free parameters, the coalescence model calculations nicely reproduce the p_T -spectra of deuterons measured by the STAR Collaboration at 0-10%, 10-20%, 20-40% and 40-60% centrality bins in Au+Au collisions at $\sqrt{s_{NN}} = 7.7 - 200$ GeV.

Figure 2 shows the rapidity distribution dN/dy of protons, deuterons, and tritons in 0-10% Au+Au collisions at $\sqrt{s_{NN}} = 7.7 - 200$ GeV. It shows that our model calculations give an excellent description of the STAR data at mid-rapidity. For the proton yield at mid-rapidity, it is determined in the (3+1)D MUSIC model by the interplay between the initial baryon stopping and thermal production at chemical freeze-out. At low collision energies, the initial baryon stopping and baryon current evolution in the hydrodynamic phase are more important than thermal production at particalization, resulting in a larger proton yield as observed in experiments. The calculated dN/dy of deuterons and tritons also show a similar trend with respect to the change in collision energies, which are again consistent with the STAR data. For the predicted shape of the dN/dy of protons, deuterons and tritons at $\sqrt{s_{NN}}=7.7-200$ GeV, it becomes wider with increasing collision energy, which can be tested in upcoming experimental measurements.

In the upper panel (a) of Fig. 3, we show the the atomic mass (m_A , $A = 1, 2, 3$ for proton, deuteron and triton)

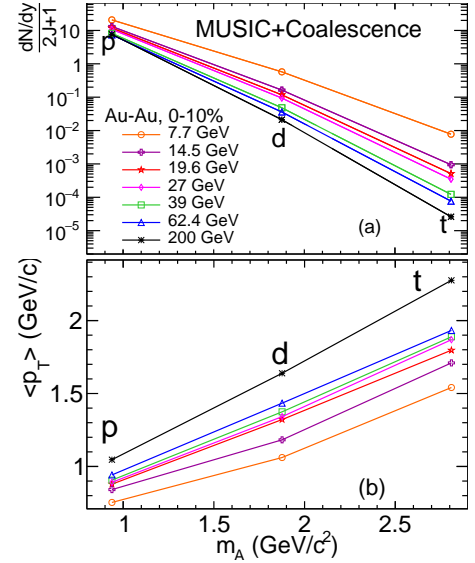


FIG. 3. (Color online) The atomic mass dependence of dN/dy (upper panel) and $\langle p_T \rangle$ (lower panel) of protons, deuterons, and tritons in 0-10% Au + Au collisions.

dependence of the rapidity distribution per degree of freedom, $\frac{dN/dy}{2J+1}$ in 0-10% Au+Au collisions at $\sqrt{s_{NN}}=7.7-200$ GeV. An exponentially decreasing $\frac{dN/dy}{2J+1}$ with the atomic mass is observed as expected from the nucleon coalescence model, in which the binding energies of produced light nuclei are ignored. The lower panel (b) shows the dependence of the mean transverse momentum $\langle p_T \rangle$

on the atomic mass m_A . The $\langle p_T \rangle$ increases with increasing m_A because light nuclei are produced in the coalescence model from nucleons close in phase space, thus enhancing their momenta. Besides, larger values of $\langle p_T \rangle$ are observed with higher collision energy, which causes a stronger radial flow and thus pushes particles to larger p_T .

B. Coalescence Parameters and Light Nuclei Yield Ratios

In interpreting light nuclei production from nuclear reactions, one usually expresses the yield $d^3N_A/d^3p_A^3$ of a nucleus with the mass number $A = Z + N$ and momentum p_A in terms of the yield $d^3N_p/d^3p_p^3$ of protons with momentum p_p and the yield $d^3N_n/d^3p_n^3$ of neutrons with momentum p_n in terms of the coalescence parameter B_A as follows:

$$E_A \frac{d^3N_A}{d^3p_A^3} = B_A \left(E_p \frac{d^3N_p}{d^3p_p^3} \right)^Z \left(E_n \frac{d^3N_n}{d^3p_n^3} \right)^{A-Z} \approx B_A \left(E_p \frac{d^3N_p}{d^3p_p^3} \right)^A \Big|_{\vec{p}_p=\vec{p}_n=\vec{p}_A}, \quad (6)$$

where $E_{p,n}$ are the proton and neutron energies. The coalescence parameter B_A ($A=2,3$) contains information on the freeze-out properties of the nucleon emission source, i.e., $B_A \propto V_{\text{eff}}^{1-A}$ with V_{eff} being the effective volume of the nucleon emission source [16–18, 70].

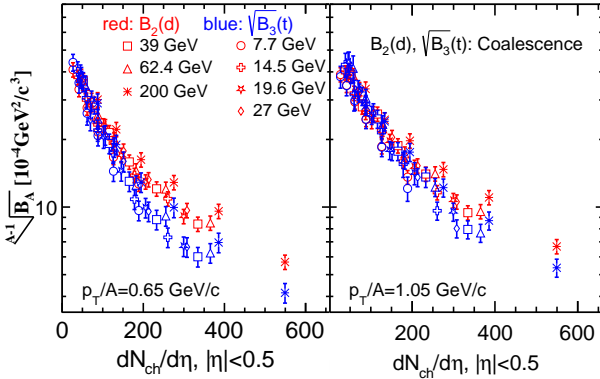


FIG. 4. (Color online) Multiplicity dependence of the coalescence parameters $B_2(d)$ and $\sqrt{B_3(t)}$ at $p_T/A = 0.65$ GeV/c and $p_T/A = 1.05$ GeV/c in Au+Au collisions from 0-10% to 50-60% centrality bins, with $A = 2$ for deuterons and $A = 3$ for tritons. The $B_2(d)$ and $\sqrt{B_3(t)}$ from our model calculations decrease monotonically with increasing multiplicity, and this is because the size of the nucleon emission source increases monotonically with increasing multiplicity. It is found the $\sqrt{B_3(t)}$

Figure 4 shows the multiplicity dependence of the coalescence parameters $B_2(d)$ and $\sqrt{B_3(t)}$ at $p_T/A=0.65$ GeV/c (left) and $p_T/A=1.05$ GeV/c (right) in Au+Au collisions from 0-10% to 50-60% centrality bins, with $A = 2$ for deuterons and $A = 3$ for tritons. The $B_2(d)$ and $\sqrt{B_3(t)}$ from our model calculations decrease monotonically with increasing multiplicity, and this is because the size of the nucleon emission source increases monotonically with increasing multiplicity. It is found the $\sqrt{B_3(t)}$

decreases more rapidly than $B_2(d)$ as a function of multiplicity. Specifically, the values of $\sqrt{B_3(t)}$ are very close to $B_2(d)$ at low multiplicities, but they start to deviate when $dN_{ch}/d\eta > 200$, which can be attributed to the different deuteron and triton sizes [70]. This is also consistent with the multiplicity dependence of the yield ratio $N_t N_p / N_d^2$ (see below). The slightly smaller coalescence parameters at $p_T/A=0.65$ GeV/c than those at $p_T/A=1.05$ GeV/c is consistent with the decreasing correlation lengths (HBT radii) with mean pair transverse momentum extracted in the STAR experiments [71]. For a fixed multiplicity, the coalescence parameter is systematically larger at a higher collision energy. For example, at $dN_{ch}/d\eta \sim 250$, the $B_2(d)$ in collisions at $\sqrt{s_{NN}}=200$ GeV is clearly greater than that at $\sqrt{s_{NN}}=14.5$ GeV. This is attributed to the stronger collective expansion at the higher collision energy, which would decrease the effective volume at kinetic freeze-out [71].

Recently, the yield ratio of light nuclei, $N_t N_p / N_d^2$, has been proposed as a sensitive probe to the critical point of QCD phase diagram [39, 40, 72–75]. The measured $N_t N_p / N_d^2$ in 0-10% central Au+Au collisions by the STAR Collaboration shows a clear non-monotonic behavior with a peak located around $\sqrt{s_{NN}} = 20$ GeV, which might indicate a non-trivial collision energy dependence of the baryon density fluctuations [62]. Due to non-negligible deuteron and triton sizes comparing to the size of the nucleon emission source, the production of light nuclei in the coalescence model is expected to be suppressed in collisions of low multiplicity, such as in peripheral AA collisions and pp collisions [17, 45, 70]. For thermal equilibrated and spherical Gaussian nucleon emission source, the double ratio, $N_t N_p / N_d^2$, in the coalescence model can be derived analytically [45], and it can be expressed as,

$$\frac{N_t N_p}{N_d^2} = \frac{4}{9} \left(\frac{1 + \frac{2r_d^2}{3R^2}}{1 + \frac{r_t^2}{2R^2}} \right)^3 = \frac{4}{9} \left(1 + \frac{\frac{4}{3}r_d^2 - r_t^2}{2R^2 + r_t^2} \right)^3, \quad (7)$$

with R being the radius of the spherical emission source and the factor $4/9$ comes from the Gaussian parameterization of the nucleon distributions. Eq. (7) clearly shows that the double ratio $N_t N_p / N_d^2$ has an asymptotic value of $4/9$ when $R \gg r_d, r_t$. Since $(2/\sqrt{3})r_d = 2.26$ fm is greater than $r_t = 1.59$ fm, the yield ratio would increase with decreasing source size and thus the particle multiplicity in heavy-ion collisions ($R \propto (dN_{ch}/d\eta)^{1/3}$), independent of its temperature and baryon chemical potential. Hence, this double ratio is also a good probe to the difference between deuteron and triton sizes. The size effects would be even stronger for hypernuclei due to their larger sizes [45].

Figure 5 shows the $N_t N_p / N_d^2$ ratio obtained from our model study as a function of the multiplicity in Au+Au at $\sqrt{s_{NN}}=7.7$ -200 GeV and Pb+Pb at $\sqrt{s_{NN}}=2.76$ TeV [31, 43, 50, 51, 76]. Besides those obtained from the hybrid MUSIC and VISHNU models, which are shown by symbols, we also include results from the AMPT model. The

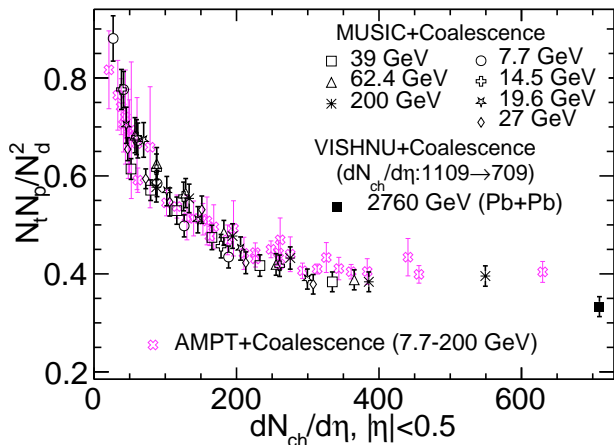


FIG. 5. (Color online) Multiplicity dependence of the yield ratio $N_t N_p / N_d^2$ in Au+Au collisions at $\sqrt{s_{NN}} = 7.7 - 200$ GeV and Pb+Pb collisions at $\sqrt{s_{NN}} = 2.76$ TeV calculated from the nucleon coalescence model using kinetically freeze-out nucleons from the MUSIC, VISHNU and AMPT models.

$N_t N_p / N_d^2$ shows a clear monotonically decrease with increasing multiplicity, and results from different model calculations are consistent with each other. More importantly, the $N_t N_p / N_d^2$ from different collision centralities and energies almost lie on the same curve. This scaling behavior in the multiplicity dependence indicates that the double ratio $N_t N_p / N_d^2$ is insensitive to the baryon density or the collective flow effect. For central Pb+Pb collisions at $\sqrt{s_{NN}} = 2.76$ TeV, the $N_t N_p / N_d^2$ from the VISHNU + coalescence model in Refs. [31, 76] is close to the value at central Au+Au collisions at 200 GeV in the present study using the MUSIC+coalescence model. However, the recent ALICE measurement of the $N_3 N_p / N_d^2$ ratio in central Pb+Pb at $\sqrt{s_{NN}} = 2.76$ TeV reaches a value around 0.9 [10], which is much larger than the theoretical value of about 0.33 from Refs. [31, 76]. Although the uncertainty in the ALICE data is still large, the almost factor of three difference between the coalescence model calculation and the experimental data at LHC needs to be understood in the future. We note that the thermal model gives an opposite behavior in the multiplicity dependence of $N_t N_p / N_d^2$, i.e., it increases with increasing multiplicity [20, 21]. As Eq.(7) indicates, the larger $N_t N_p / N_d^2$ at lower multiplicity is due to the larger deuteron than triton radius. This enhancement in the value of $N_t N_p / N_d^2$ would disappear if the deuteron and triton radii were similar. Indeed, changing the triton radius to that of deuteron in the coalescence model calculations using nucleons from the AMPT model, we have obtained an almost constant value of about 0.33 for all particle multiplicities. This result strongly indicates the importance of the size effect on coalescence production of light nuclei in heavy-ion collisions. The upcoming measurements of $N_t N_p / N_d^2$ as a function of multiplicity would thus help discriminate different production mechanisms of light nuclei in heavy-ion collisions. We would like to

point out that neither the hydrodynamic nor the AMPT model in our study includes any dynamical density fluctuations related to the critical point or first-order phase transition of the QCD matter. Therefore, our results can serve as the baseline predictions for the yield ratio of light nuclei in the search for the possible QCD critical point from experimental beam energy scan of heavy-ion collisions.

IV. SUMMARY

In this paper, we have presented the multiplicity dependence of light nuclei production in Au+Au collisions at $\sqrt{s_{NN}} = 7.7 - 200$ GeV and Pb+Pb collision at $\sqrt{s_{NN}} = 2.76$ TeV by using the nucleon coalescence model with the phase-space distributions of protons and neutrons at kinetic freeze-out taken from the MUSIC, VISHNU or AMPT model. The model results nicely reproduce the measured p_T -spectra of protons and deuterons in 0-10%, 10-20%, 20-40% and 40-60% Au+Au collisions at $\sqrt{s_{NN}} = 7.7 - 200$ GeV and 0-20% Pb+Pb collisions at $\sqrt{s_{NN}} = 2.76$ TeV. The coalescence parameters $B_2(d)$ and $\sqrt{B_3(t)}$ are found to decrease monotonically with increasing multiplicity. Furthermore, the yield ratio $N_t N_p / N_d^2$ from 7.7 GeV to 2.76 TeV exhibit a scaling behavior, i.e., decreasing monotonically with increasing charged-particle multiplicity. This scaling behavior can be used to validate the production mechanism of light nuclei and to extract the sizes of light nuclei, particularly those of hypernuclei, in relativistic heavy-ion collisions. Since the MUSIC, VISHNU or AMPT models used in the present study cannot generate any dynamical density fluctuations related to the critical point and first-order phase transitions of QCD at all collision energies, our model results can serve as a baseline against which one can compare the experimental data from the beam energy scan of heavy-ion collisions to search for the critical point in the QCD phase diagram.

ACKNOWLEDGEMENTS

We thank Chun Shen for helpful discussions. This work is supported in part by the National Key Research and Development Program of China (Grant No. 2020YFE0202002 and 2018YFE0205201), the National Natural Science Foundation of China (Grant No. 11828501, 11890711, 11861131009, 11935007, 11221504 and 11890714), US DOE under grant No. DE-AC02-05CH11231, US NSF under grant Nos. ACI-1550300 and OAC-2004571, 5th Fundamental Research Funds for Central Universities in China and the UCB-CCNU Collaboration Grant. K. J. S. and C. M. K. were supported in part by the US Department of Energy under Award No. DE-SC0015266 and the Welch Foundation under Grant No. A-1358.

-
- [1] G. Ambrosini et al. (NA52 (NEWMASS)), Phys. Lett. **B417**, 202 (1998).
 - [2] T. A. Armstrong et al. (E864), Phys. Rev. **C61**, 064908 (2000), nucl-ex/0003009.
 - [3] C. Adler et al. (STAR), Phys. Rev. Lett. **87**, 262301 (2001), [Erratum: Phys. Rev. Lett. **87**, 279902 (2001)], nucl-ex/0108022.
 - [4] S. S. Adler et al. (PHENIX), Phys. Rev. Lett. **94**, 122302 (2005), nucl-ex/0406004.
 - [5] I. Arsene et al. (BRAHMS), Phys. Rev. **C83**, 044906 (2011), 1005.5427.
 - [6] B. I. Abelev et al. (STAR), Science **328**, 58 (2010), 1003.2030.
 - [7] H. Agakishiev et al. (STAR), Nature **473**, 353 (2011), [Erratum: Nature **475**, 412 (2011)], 1103.3312.
 - [8] N. Yu (STAR), Nucl. Phys. **A967**, 788 (2017), 1704.04335.
 - [9] J. Adam et al. (ALICE), Phys. Lett. **B754**, 360 (2016), 1506.08453.
 - [10] J. Adam et al. (ALICE), Phys. Rev. **C93**, 024917 (2016), 1506.08951.
 - [11] T. Anticic et al. (NA49), Phys. Rev. **C94**, 044906 (2016), 1606.04234.
 - [12] S. Acharya et al. (ALICE), Eur. Phys. J. **C77**, 658 (2017), 1707.07304.
 - [13] J. Chen, D. Keane, Y.-G. Ma, A. Tang, and Z. Xu, Phys. Rept. **760**, 1 (2018), 1808.09619.
 - [14] P. Braun-Munzinger and B. Dönigus, Nucl. Phys. A **987**, 144 (2019), 1809.04681.
 - [15] B. Dönigus, Int. J. Mod. Phys. E **29**, 2040001 (2020), 2004.10544.
 - [16] L. P. Csernai and J. I. Kapusta, Phys. Rept. **131**, 223 (1986).
 - [17] R. Scheibl and U. W. Heinz, Phys. Rev. **C59**, 1585 (1999), nucl-th/9809092.
 - [18] F. Bellini and A. P. Kalweit, Phys. Rev. **C99**, 054905 (2019), 1807.05894.
 - [19] A. Andronic, P. Braun-Munzinger, K. Redlich, and J. Stachel, Nature **561**, 321 (2018), 1710.09425.
 - [20] V. Vovchenko, B. Dönigus, and H. Stoecker, Phys. Lett. **B785**, 171 (2018), 1808.05245.
 - [21] V. Vovchenko, B. Dönigus, B. Kardan, M. Lorenz, and H. Stoecker, Phys. Lett. **B**, 135746 (2020), [Phys. Lett. **B809**, 135746 (2020)], 2004.04411.
 - [22] R. Mattiello, A. Jahns, H. Sorge, H. Stoecker, and W. Greiner, Phys. Rev. Lett. **74**, 2180 (1995).
 - [23] R. Mattiello, H. Sorge, H. Stoecker, and W. Greiner, Phys. Rev. **C55**, 1443 (1997), nucl-th/9607003.
 - [24] L.-W. Chen, C. M. Ko, and B.-A. Li, Phys. Rev. **C68**, 017601 (2003), nucl-th/0302068.
 - [25] L.-W. Chen, C. M. Ko, and B.-A. Li, Nucl. Phys. **A729**, 809 (2003), nucl-th/0306032.
 - [26] N. Shah, Y. G. Ma, J. H. Chen, and S. Zhang, Phys. Lett. **B754**, 6 (2016), 1511.08266.
 - [27] K.-J. Sun and L.-W. Chen, Phys. Lett. **B751**, 272 (2015), 1509.05302.
 - [28] K.-J. Sun and L.-W. Chen, Phys. Rev. **C93**, 064909 (2016), 1512.00692.
 - [29] A. S. Botvina, J. Steinheimer, and M. Bleicher, Phys. Rev. **C96**, 014913 (2017), 1706.08335.
 - [30] X. Yin, C. M. Ko, Y. Sun, and L. Zhu, Phys. Rev. **C95**, 054913 (2017), 1703.09383.
 - [31] W. Zhao, L. Zhu, H. Zheng, C. M. Ko, and H. Song, Phys. Rev. **C98**, 054905 (2018), 1807.02813.
 - [32] W. Zhao, C. Shen, C. M. Ko, Q. Liu, and H. Song, Phys. Rev. **C102**, 044912 (2020), 2009.06959.
 - [33] M. Kozhevnikova, Y. B. Ivanov, I. Karpenko, D. Blaschke, and O. Rogachevsky, Phys. Rev. **C103**, 044905 (2021), 2012.11438.
 - [34] Y. Oh, Z.-W. Lin, and C. M. Ko, Phys. Rev. **C80**, 064902 (2009), 0910.1977.
 - [35] D. Oliinychenko, L.-G. Pang, H. Elfner, and V. Koch, Phys. Rev. **C99**, 044907 (2019), 1809.03071.
 - [36] L. Adamczyk et al. (STAR), Phys. Rev. **C94**, 034908 (2016), 1601.07052.
 - [37] J. Adam et al. (STAR), Phys. Rev. **C99**, 064905 (2019), 1903.11778.
 - [38] D. Zhang (STAR), Nucl. Phys. A **1005**, 121825 (2021), 2002.10677.
 - [39] K.-J. Sun, L.-W. Chen, C. M. Ko, and Z. Xu, Phys. Lett. **B774**, 103 (2017), 1702.07620.
 - [40] K.-J. Sun, L.-W. Chen, C. M. Ko, J. Pu, and Z. Xu, Phys. Lett. **B781**, 499 (2018), 1801.09382.
 - [41] N. Yu, D. Zhang, and X. Luo, Chin. Phys. **C44**, 014002 (2020), 1812.04291.
 - [42] H. Liu, D. Zhang, S. He, K.-j. Sun, N. Yu, and X. Luo, Phys. Lett. B **805**, 135452 (2020), 1909.09304.
 - [43] K.-J. Sun and C. M. Ko (2020), 2005.00182.
 - [44] X. Deng and Y. Ma, Phys. Lett. B **808**, 135668 (2020), 2006.12337.
 - [45] K.-J. Sun, C. M. Ko, and B. Donigus, Phys. Lett. **B792**, 132 (2019), 1812.05175.
 - [46] C. Shen and B. Schenke, Phys. Rev. **C97**, 024907 (2018), 1710.00881.
 - [47] C. Shen and B. Schenke, PoS **CPOD2017**, 006 (2018), 1711.10544.
 - [48] G. S. Denicol, C. Gale, S. Jeon, A. Monnai, B. Schenke, and C. Shen, Phys. Rev. **C98**, 034916 (2018), 1804.10557.
 - [49] C. Shen and B. Schenke, Nucl. Phys. **A982**, 411 (2019), 1807.05141.
 - [50] Z.-W. Lin, C. M. Ko, B.-A. Li, B. Zhang, and S. Pal, Phys. Rev. C **72**, 064901 (2005), nucl-th/0411110.
 - [51] C. Shen and S. Alzhrani, Phys. Rev. **C102**, 014909 (2020), 2003.05852.
 - [52] G. Ropke, Phys. Rev. **C79**, 014002 (2009), 0810.4645.
 - [53] L. Adamczyk et al. (STAR), Phys. Rev. Lett. **121**, 032301 (2018), 1707.01988.
 - [54] S. S. Adler et al. (PHENIX), Phys. Rev. **C69**, 034909 (2004), nucl-ex/0307022.
 - [55] B. Schenke, S. Jeon, and C. Gale, Phys. Rev. Lett. **106**, 042301 (2011), 1009.3244.
 - [56] B. Schenke, S. Jeon, and C. Gale, Phys. Rev. **C82**, 014903 (2010), 1004.1408.
 - [57] J.-F. Paquet, C. Shen, G. S. Denicol, M. Luzum, B. Schenke, S. Jeon, and C. Gale, Phys. Rev. C **93**, 044906 (2016), 1509.06738.
 - [58] A. Monnai, B. Schenke, and C. Shen, Phys. Rev. **C100**, 024907 (2019), 1902.05095.
 - [59] S. Bass et al., Prog. Part. Nucl. Phys. **41**, 255 (1998), nucl-th/9803035.

- [60] M. Bleicher et al., J. Phys. **G25**, 1859 (1999), hep-ph/9909407.
- [61] We use the official UrQMD v3.4 and set it up to run as the afterburner mode, https://bitbucket.org/Chunshen1987/urqmd_afterburner/src/master/.
- [62] D. Zhang (STAR), JPS Conf. Proc. **32**, 010069 (2020), 1909.07028.
- [63] V. Greco, C. M. Ko, and P. Levai, Phys. Rev. **C68**, 034904 (2003), nucl-th/0305024.
- [64] V. Greco, C. M. Ko, and R. Rapp, Phys. Lett. **B595**, 202 (2004), nucl-th/0312100.
- [65] R. J. Fries, B. Muller, C. Nonaka, and S. A. Bass, Phys. Rev. **C68**, 044902 (2003), nucl-th/0306027.
- [66] R. C. Hwa and C. B. Yang, Phys. Rev. **C70**, 024905 (2004), nucl-th/0401001.
- [67] R. J. Fries, V. Greco, and P. Sorensen, Ann. Rev. Nucl. Part. Sci. **58**, 177 (2008), 0807.4939.
- [68] W. Zhao, C. M. Ko, Y.-X. Liu, G.-Y. Qin, and H. Song, Phys. Rev. Lett. **125**, 072301 (2020), 1911.00826.
- [69] W. Zhao, W. Ke, W. Chen, T. Luo, and X.-N. Wang (2021), 2103.14657.
- [70] R.-Q. Wang, F.-L. Shao, and J. Song (2020), 2007.05745.
- [71] L. Adamczyk et al. (STAR), Phys. Rev. **C92**, 014904 (2015), 1403.4972.
- [72] K.-J. Sun, F. Li, and C. M. Ko, Phys. Lett. B **816**, 136258 (2021), 2008.02325.
- [73] K.-J. Sun, C. M. Ko, F. Li, J. Xu, and L.-W. Chen (2020), 2006.08929.
- [74] E. Shuryak and J. M. Torres-Rincon, Phys. Rev. **C100**, 024903 (2019), 1805.04444.
- [75] E. Shuryak and J. M. Torres-Rincon, Phys. Rev. C **101**, 034914 (2020), 1910.08119.
- [76] W. Zhao, H.-j. Xu, and H. Song, Eur. Phys. J. **C77**, 645 (2017), 1703.10792.